

Eigo Otsuji · Yoshiaki Kuriu · Kazuma Okamoto  
Daisuke Ichikawa · Akeo Hagiwara · Hiroto Ito  
Tsunehiko Nishimura · Hisakazu Yamagishi

## Monoclonal antibody A7 coupled to magnetic particles as a contrast enhancing agent for magnetic resonance imaging of human colorectal carcinoma

Received: 20 June 2003 / Accepted: 6 June 2005 / Published online: 5 November 2005  
© Springer-Verlag 2005

**Abstract** *Background:* Local recurrence, the most frequent pattern of recurrence of rectal carcinoma, is almost always fatal. The difficulty of diagnosing local recurrence contributes importantly to the poor prognosis. *Methods:* We coupled monoclonal antibody (Mab) A7, which reacts specifically with human colorectal carcinoma, to ferromagnetic lignosite (FML) particles to distinguish rectal carcinoma from other tissues by magnetic resonance (MR) imaging. We examined retention of immunoreactivity by the A7-FML complexes in vitro, and also their distribution in vivo according to radiolabeling and MR imaging when injected into nude mice bearing human colorectal carcinoma xenografts. *Results:* A7-FML retained binding activity nearly identical to that of Mab A7. Significantly more  $^{125}\text{I}$ -labeled A7-FML accumulated in engrafted tumors than did  $^{125}\text{I}$ -labeled normal mouse IgG-FML complexes ( $P < 0.05$ ). A7-FML disappeared rapidly from the blood. Normal tissues accumulated less  $^{125}\text{I}$ -labeled A7-FML than tumors; this accumulation decreased linearly with time. In MR imaging, signal intensity was reduced in the tumor by the injection of A7-FML. *Conclusions:* A7-FML is potentially useful as a MR contrast enhancing agent for human colorectal carcinoma xenografts implanted subcutaneously.

**Keywords** Magnetic resonance imaging · Colorectal cancer · Contrast agent · Monoclonal antibody · Ferromagnetic particles

E. Otsuji (✉) · Y. Kuriu · K. Okamoto · D. Ichikawa  
A. Hagiwara · H. Yamagishi  
Department of Surgery, Kyoto Prefectural University of Medicine,  
Kawaramachi Hirokoji Kamigyo-ku, Kyoto, 602-8566, Japan  
E-mail: otsuji@koto.kpu-m.ac.jp  
Tel.: +81-75-2515527  
Fax: +81-75-2515522

H. Ito · T. Nishimura  
Department of Radiology, Kyoto Prefectural  
University of Medicine, Kawaramachi Hirokoji Kamigyo-ku,  
Kyoto, 602-8566, Japan

### Introduction

The recurrence rate of rectal carcinoma is approximately 30% even after curative resection is successfully attempted [7]. Local recurrence, the most frequent pattern of recurrence in rectal carcinoma, is almost always fatal. The difficulty of diagnosis of local recurrence is one among the reasons for poor prognosis. Several methods including ultrasonography (US), computed tomography (CT), magnetic resonance imaging (MR imaging), and angiography have been applied to the diagnosis of these recurrences, but in many cases detection is not possible until the recurrence is incurable.

Radioimmunoscintigraphic application of monoclonal antibody (Mab) for noninvasive detection and visualization of various targets [6, 9, 17] has grown immensely. Since the initial use of  $^{131}\text{I}$ -Mab for experimental tumor imaging [1], several trials of tumor imaging using  $^{131}\text{I}$ -,  $^{111}\text{In}$ -, and  $^{99\text{m}}\text{Tc}$ -labeled Mabs have been reported [3, 13, 14].

Conventional MR imaging has only limited ability to distinguish recurrent rectal carcinoma from other tissues; new enhanced imaging techniques are under investigation. Use of ferromagnetic particles ( $\text{Fe}_3\text{O}_4$ ) as MR imaging contrast enhancing agents have been proposed recently [5, 11, 18]. Although paramagnetic substances also have been investigated, they possess much smaller magnetic moments than ferromagnetic particles of similar size [2, 11].

We previously have produced the Mab A7 and have demonstrated that it reacts with colorectal carcinoma in a highly sensitive manner [15, 23]. Mab A7 has been used clinically as a carrier of anticancer drugs or a radiolabel [23]. In the present report Mab A7 was coupled to ferromagnetic particles to improve MR imaging discrimination between rectal carcinoma and other tissues. Our goal was to study the accumulation of both labeled and unlabeled Mab A7 coupled ferromagnetic particles in tumor and to determine if their deposition would alter resulting MR imaging signal

intensities. First, we investigated in vitro retention of radio-labeled compound using immunoreactivity assays. Second, we examined the in vivo distribution of these complexes after injection into nude mice bearing human colorectal carcinoma xenografts.

## Material and methods

### Cell line

The human colorectal carcinoma cell line, WiDr, was used in this study. WiDr cells were maintained in RPMI 1640 media supplemented with 10% fetal bovine serum (FBS)(Flow Laboratories, Inc., Rockville, MD, USA).

### Tumor xenograft

Cultured WiDr cells were harvested by EDTA treatment, washed in PBS and resuspended in PBS. Approximately  $1 \times 10^7$  viable cells were injected subcutaneously into the left flank of thymus-deficient 8-week-old nude mice (BALB/C, nu-nu, male, mean body weight: approximately 21 g) (SLC Co., Shizuoka, Japan). A tumor mass was detected in all the mice injected with WiDr cells 14 days after tumor inoculation.

### Preparation of Mab A7

Mab A7 was derived from hybridomas against human colonic carcinoma, recognizes a 42,000 Dalton glycoprotein on the cell surface. Mab A7 is an IgG<sub>1</sub> protein and has been reported to react with more than 70% of the human colonic carcinomas [10, 16, 23].

### Preparation of radiolabeled Mab A7

Radiolabeling of Mab A7 with <sup>125</sup>I (ICN Biomedicals, Inc., CA, USA) was performed by the chloramine-T method [8]. Mab A7 was labeled with <sup>125</sup>I to specific activities of 1.0 μCi/μg.

### Preparation of ferromagnetic particles

Ferromagnetic particles (FML; Georgia-Pacific, WA, USA) have a mean diameter of 10 nm, and are coated with lignosulfate. FML was stored in distilled water at room temperature until use.

### Binding of <sup>125</sup>I labeled Mab to ferromagnetic particles

Three milligrams of FML in 500 μl of phosphate-buffered saline (PBS) was added to 250 μg of <sup>125</sup>I labeled Mab A7 in 300 μl of PBS and sonicated on ice. After

blocking with bovine serum albumin to saturate additional binding sites of FML, the preparation was centrifuged at 400,000g for 15 min to separate A7-FML from free Mab A7. The pellet was washed thoroughly with 10 mM Hepes buffer at pH 7.4. FML also was bound to normal mouse IgG as a control. Approximately 40% of the antibody added initially was found to be associated with the magnetite.

### Binding of A7-FML to WiDr cells

Binding activities of A7-FML were measured by a competitive radioimmunoassay using WiDr cells. Aliquots of  $10^6$  WiDr cells were incubated with <sup>125</sup>I-labeled A7 ( $10^5$  cpm) in the presence of 5-fold serially diluted A7-FML or free A7 at 37°C for 60 min. The concentration of A7-FML or free A7 ranged from  $5^{-7}$  to 1.0 μg/ml. As a control, normal mouse IgG-FML was used instead of A7-FML or free A7. After incubation, the cell pellets were subjected to γ-scintillation counting (Auto-Gamma 5000, Packard, ILL) and the percent inhibition was calculated in comparison to the results from the control group.

### Biodistribution of <sup>125</sup>I labeled A7-FML in nude mice bearing human colorectal carcinoma xenografts

The distribution of <sup>125</sup>I labeled A7-FML was investigated in athymic nude mice bearing WiDr tumors. Fourteen days after inoculation, tumor-bearing mice were divided into two groups of 16 animals each. According to group, mice were injected intravenously with 0.7 μCi of <sup>125</sup>I-labeled A7-FML or <sup>125</sup>I-labeled normal mouse IgG-FML. Four mice from each group were killed and dissected at 2, 12, 24, 48, and 72 h after injection. After dissection the tumors, blood, and unaffected organs (lung, heart, liver, spleen, pancreas, colon, and kidney) were weighed. The tumor weight was  $131 \pm 23$  mg (mean ± SD). Radioactivity in each tissue (cpm/g) was measured using the γ-scintillation counter. To compare the specific localization of the two probes in the tumors to that in blood or normal tissues, the ratio of radioactivity in the tumor or normal tissue to that in blood was determined. These ratios were obtained by dividing the radioactivity per weight of tissue by radioactivity per weight of total blood. Student's *t* test was used to determine statistically significant differences. A *p* value < 0.05 was considered significant. Care of the animals and the experimental procedures were carried out in accordance with the Guidelines of the Institutional Animal Care and Use Committee at our institution.

### MR imaging of human colorectal carcinoma xenografted in nude mouse

Three athymic nude mice were used 14 days after inoculation of WiDr tumors. Each Tumor-bearing nude

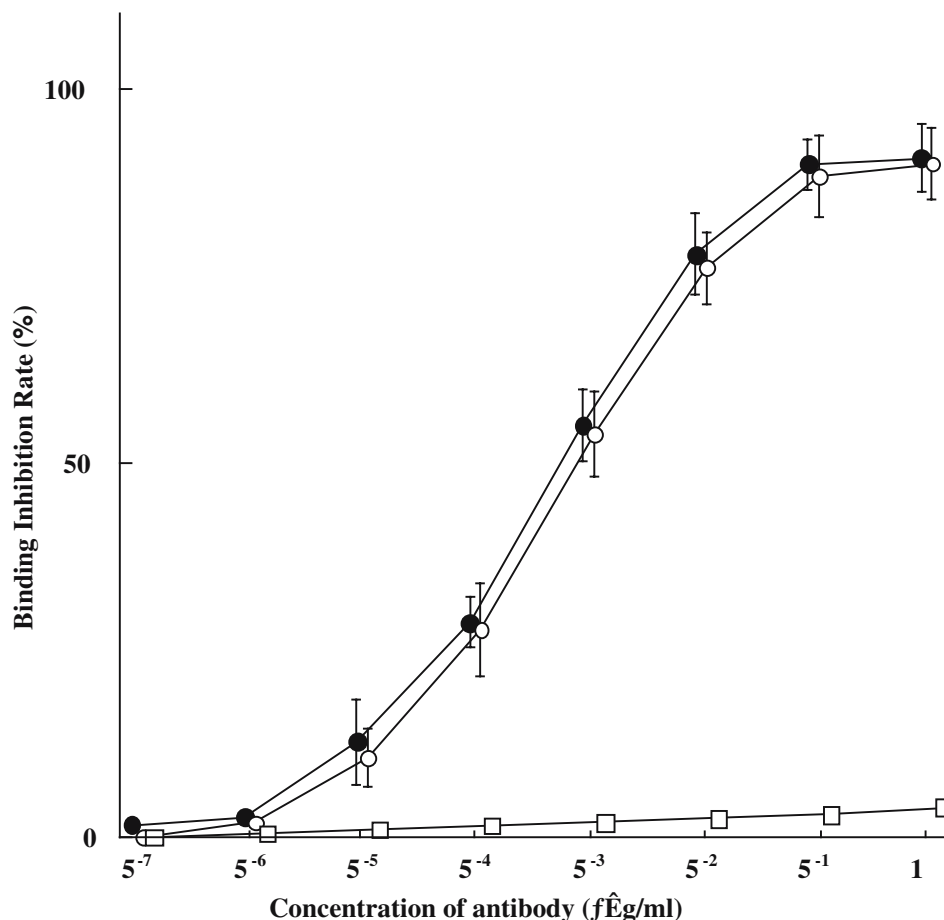
mouse was imaged before 72 h after injection of A7-FML or 72 h after injection of normal mouse IgG-FML with an MR imaging scanner (Shimadzu-Marconi Medical Systems, Japan). All MR images were obtained with 1.5 T clinical scanner with a small FOV (field of view) coil (Eclipse 1.5 T, Marconi Medical systems). These images were obtained with a T2\*-weighted gradient echo sequence. We used T2\* sequence to visualize the uptake of SPIO, because the T2\* sequence was one of the most sensitive sequence to visualize the magnetic susceptibility. These images were obtained with a T2\*-weighted gradient echo sequence with following parameters: repetition time/echo time = 323/8.9 ms, flip angle 60 degree, Bandwidth 31.2 Hz, matrix 512×512, field of view 24 cm, number of acquisition 2, slice thickness 5 mm, total slices 11, scan time 5 min30 s

## Results

### Binding activities of A7-FML to WiDr cells

As shown in Fig. 1, A7-FML retained a binding activity nearly identical to that of free Mab A7. Normal mouse IgG-FML showed no specific binding activity.

**Fig. 1** In vitro binding activity of A7-FML compared with the binding activity of Mab A7 by competitive radioimmunoassay in WiDr cells. A7-FML retained binding activity nearly identical to that of Mab A7. (open circle), A7-FML; (filled circle), Mab A7; (open square), normal mouse IgG-FML



Biodistribution of <sup>125</sup>I labeled A7-FML in nude mice bearing human colorectal carcinoma xenografts

<sup>125</sup>I-labeled A7-FML and <sup>125</sup>I-labeled normal mouse IgG-FML disappeared from blood rapidly, showing similar linear clearance curves over time (Fig. 2). Tumor accumulation of <sup>125</sup>I-labeled A7-FML increased until 24 h after injection and then decreased slowly. In contrast, tumor accumulation of <sup>125</sup>I-labeled normal mouse IgG-FML decreased with time (Fig. 3). From 2 to 72 h after injection, significantly more radiolabeled <sup>125</sup>I-labeled A7-FML accumulated in the tumor than did <sup>125</sup>I-labeled normal mouse IgG-FML ( $P < 0.05$ ). All resected normal tissues showed less accumulation of <sup>125</sup>I-labeled A7-FML than the tumors. Accumulation of <sup>125</sup>I-labeled A7-FML and <sup>125</sup>I-labeled normal mouse IgG-FML obtained from normal tissues decreased with time post injection and were similar to one another in normal tissues (Fig. 3). To examine specific localization of <sup>125</sup>I-labeled A7-FML and <sup>125</sup>I-labeled normal mouse IgG-FML in tumors, the ratio of radioactivity in normal and tumor tissues to that in blood was determined. The tumor tissue/blood ratio of <sup>125</sup>I labeled A7-FML increased rapidly in a time-dependent manner to  $2.59 \pm 0.21$  at 72 h after injection, while the tissue/blood

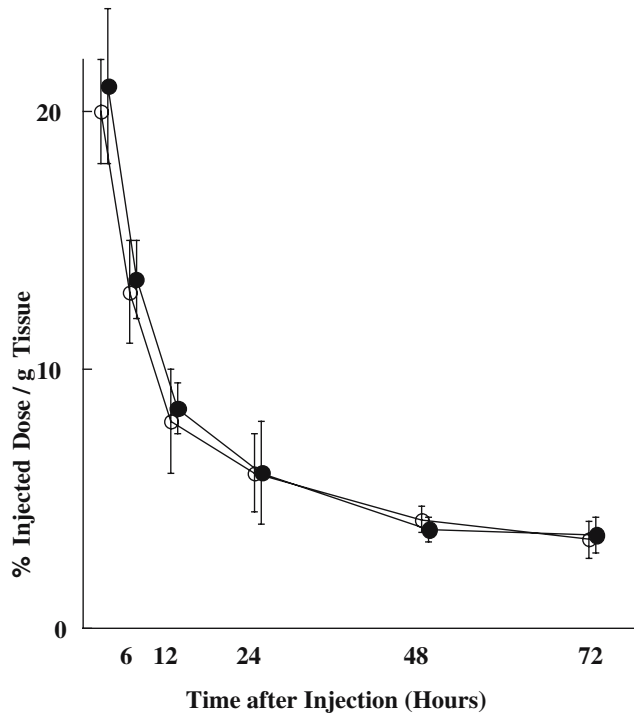


**Fig. 2** Intravenously injected  $^{125}\text{I}$ -labeled A7-FML (open circle) or  $^{125}\text{I}$ -labeled normal mouse IgG-FML (filled circle) disappeared rapidly from the blood of mice, showing similar linear clearance curves over time. Points are means, and bars are SD

ratio for normal organs was low (Table 1). In contrast, the tumor tissue/blood ratio of  $^{125}\text{I}$ -labeled normal mouse IgG-FML was lower than that of  $^{125}\text{I}$ -labeled A7-FML (Table 2).

## MR imaging of xenografted human colorectal carcinoma in nude mice

Signal intensity was reduced at the periphery of the tumor by injection of A7-FML. In contrast, signal intensity of the tumor was not changed by injection of normal mouse IgG-FML (Fig. 4).

## Discussion

Contrast agents are used to increase information content in diagnostic images. Enhanced CT has been used to differentiate tumor from normal tissue in the abdominal cavity. Although CT with a contrast agent can help to diagnose rectal carcinoma, recurrence of rectal carcinoma is often difficult to differentiate from postoperative granulation tissue. Conventional MR imaging has similar limitations. Accordingly, recurrence of rectal carcinoma often cannot be detected at a curable stage.

Magnetic resonance imaging research has emphasized the development of paramagnetic molecules that act mainly to decrease spin-lattice ( $T_1$ ) relaxation times. In particular, gadolinium-diethyl-enetriaminepentaacetic acid (DTPA) has been used [4]. Use of ferromagnetic particles as contrast agents in MR imaging has been proposed recently [5, 11, 18]. The cooperative alignment of the atomic magnetic moments in ferromagnetic particles renders their total magnetic moment approximately ten times larger than that obtained with comparable paramagnetic materials [18]. Ferromagnetic particles, therefore, should reduce the water relaxation

**Table 1** Tissue/blood ratio of radioactivity for tumor and normal tissues after injection of  $^{125}\text{I}$ -labeled A7 FML

Hours after injection	2	6	12	24	48	72
Tumor	$0.20 \pm 0.08$	$0.37 \pm 0.13$	$0.54 \pm 0.09$	$0.93 \pm 0.18$	$1.64 \pm 0.19$	$2.59 \pm 0.11$
Lung	$0.11 \pm 0.01$	$0.13 \pm 0.01$	$0.16 \pm 0.04$	$0.21 \pm 0.04$	$0.36 \pm 0.05$	$0.53 \pm 0.09$
Heart	$0.14 \pm 0.01$	$0.16 \pm 0.02$	$0.21 \pm 0.03$	$0.24 \pm 0.03$	$0.32 \pm 0.05$	$0.31 \pm 0.06$
Liver	$0.18 \pm 0.03$	$0.21 \pm 0.04$	$0.26 \pm 0.04$	$0.25 \pm 0.05$	$0.34 \pm 0.12$	$0.40 \pm 0.15$
Spleen	$0.16 \pm 0.03$	$0.20 \pm 0.03$	$0.23 \pm 0.03$	$0.25 \pm 0.05$	$0.33 \pm 0.10$	$0.33 \pm 0.09$
Pancreas	$0.08 \pm 0.02$	$0.10 \pm 0.02$	$0.10 \pm 0.04$	$0.12 \pm 0.05$	$0.20 \pm 0.04$	$0.26 \pm 0.1$
Colon	$0.07 \pm 0.01$	$0.09 \pm 0.02$	$0.10 \pm 0.03$	$0.10 \pm 0.04$	$0.16 \pm 0.03$	$0.22 \pm 0.10$
Kidney	$0.12 \pm 0.03$	$0.15 \pm 0.02$	$0.19 \pm 0.03$	$0.21 \pm 0.04$	$0.31 \pm 0.08$	$0.39 \pm 0.10$

**Table 2** Tissue/blood ratio of radioactivity for tumor and normal tissues to that in the blood after injection of  $^{125}\text{I}$ -labeled normal mouse IgG FML

Hours after injection	2	6	12	24	48	72
Tumor	$0.15 \pm 0.08$	$0.19 \pm 0.11$	$0.22 \pm 0.13$	$0.25 \pm 0.09$	$0.30 \pm 0.13$	$0.39 \pm 0.14$
Lung	$0.11 \pm 0.02$	$0.13 \pm 0.02$	$0.15 \pm 0.02$	$0.21 \pm 0.03$	$0.32 \pm 0.03$	$0.49 \pm 0.09$
Heart	$0.14 \pm 0.01$	$0.17 \pm 0.01$	$0.19 \pm 0.03$	$0.23 \pm 0.03$	$0.33 \pm 0.09$	$0.34 \pm 0.07$
Liver	$0.18 \pm 0.02$	$0.22 \pm 0.03$	$0.26 \pm 0.04$	$0.27 \pm 0.09$	$0.34 \pm 0.10$	$0.41 \pm 0.11$
Spleen	$0.15 \pm 0.02$	$0.19 \pm 0.03$	$0.22 \pm 0.03$	$0.25 \pm 0.03$	$0.32 \pm 0.11$	$0.36 \pm 0.10$
Pancreas	$0.09 \pm 0.01$	$0.09 \pm 0.02$	$0.08 \pm 0.01$	$0.10 \pm 0.04$	$0.17 \pm 0.04$	$0.22 \pm 0.06$
Colon	$0.07 \pm 0.01$	$0.09 \pm 0.02$	$0.10 \pm 0.02$	$0.09 \pm 0.04$	$0.14 \pm 0.03$	$0.17 \pm 0.07$
Kidney	$0.13 \pm 0.02$	$0.15 \pm 0.03$	$0.17 \pm 0.03$	$0.21 \pm 0.04$	$0.26 \pm 0.05$	$0.30 \pm 0.09$

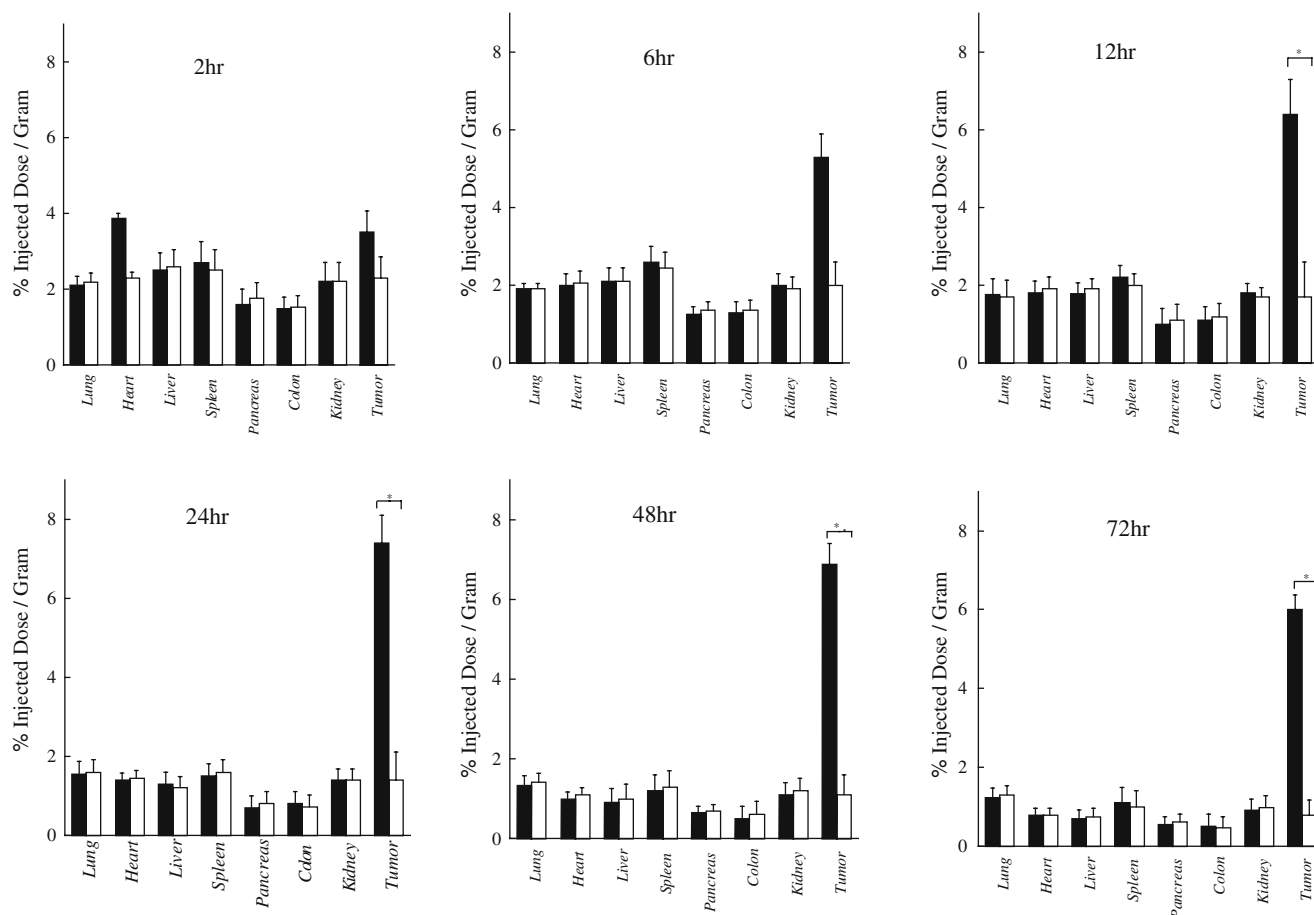


**Fig. 3** Accumulation of  $^{125}\text{I}$ -labeled A7-FML or  $^{125}\text{I}$ -labeled normal mouse IgG-FML in WiDr tumor xenografts and normal tissues from 2 to 72 h after injection. From 12 to 72 h after injection, significantly more radiolabeled  $^{125}\text{I}$ -labeled A7-FML accumulated in tumors than did  $^{125}\text{I}$ -labeled normal mouse

IgG-FML ( $P < 0.05$ ). In contrast,  $^{125}\text{I}$ -labeled A7-FML and  $^{125}\text{I}$ -labeled normal mouse IgG-FML showed similar accumulation in normal tissues. Closed column A7-FML, open column normal mouse IgG-FML, bar SD

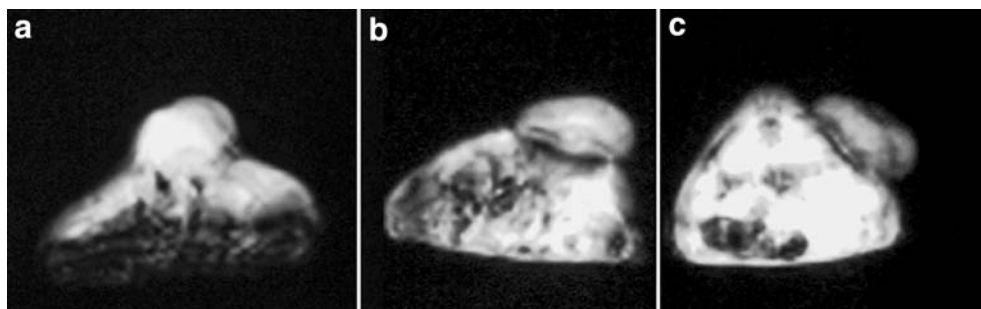
times more than paramagnetic materials. For this reason we coupled Mab A7 to FML, a ferromagnetic particle.

Molday et al. [12] reported cell separation using antibody-coated magnetic microspheres consisting of ferromagnetic colloidal particles coated with methacrylate copolymers. Labeled cells were separated from unlabeled cells by retention in magnetic fields. Coating of ferromagnetic particles with Mabs directed against carcinomas for use as selective contrast agents in MR imaging would represent a logical extension of their experiments. In our previous study, Mab A7 reacted

with more than 70% of human colorectal carcinoma specimens [23]. Moreover, the antigen recognized by Mab A7 appears to be rare, or present in only very small amounts, in sera from patients with carcinoma [15]. In this study we successfully coupled Mab A7 with FML, finding antibody activity to be retained almost completely.

Recently, magnetic substances have been used to improve the diagnostic quality of MR imaging of liver [19, 21, 22] and lymph nodes [24]. In these instances, phagocytotic cells of the reticuloendothelial system trap

**Fig. 4** Signal intensity was reduced at the periphery of the tumor by injection of A7-FML (c) compared with an image without injection (a). In contrast, signal intensity did not decrease when normal mouse IgG-FML was injected (b)



the magnetic particles. To be used as a contrast agent for MR imaging of rectal carcinoma, magnetic particles must escape elimination by phagocytotic cells and then selectively accumulate in tumors. Small particle size is advantageous for preventing rapid elimination by the reticuloendothelial system. Furthermore, particles of a diameter larger than 50 nm would not pass freely through capillary fenestrations to reach tumor antigens [20]. The mean diameter of FML is approximately 10 nm, and we found only negligible trapping in reticuloendothelial organs. A significantly larger amount of  $^{125}\text{I}$ -labeled A7-FML accumulated in the tumor than in blood or normal tissues. Furthermore, 9.8 times more  $^{125}\text{I}$ -labeled A7-FML accumulated in tumor than normal colorectal tissue 72 h after injection (Fig. 3). A significantly larger amount of  $^{125}\text{I}$ -labeled A7-FML accumulated in the tumor than  $^{125}\text{I}$ -labeled normal mouse IgG-FML (Fig. 3). These results suggest that localization of  $^{125}\text{I}$ -labeled A7-FML to colorectal carcinoma resulted from specific antigen-antibody binding. Based on these results, A7-FML may be potentially useful as an MR contrast enhancing agent of MR imaging of recurrent rectal carcinoma.

**Acknowledgements** This work was supported by Foundation for Promotion of Cancer Research in Japan.

## References

- Ballou B, Levine G, Hakala TR, Solter D (1979) Tumor location detected with radioactively labeled monoclonal antibody and external scintigraphy. *Science* 206:844–847
- Borris TJ, Weber CR (1999) Ferromagnetic MRI artifact secondary to a previous mandibular modified condylotomy. *Br J Oral Maxillofac Surg* 37:104–105
- Brouwers AH, Dorr U, Lang O, Boerman OC, Oyen WJ, Steffens MG, Oosterwijk E, Mergenthaler HG, Bihl H, Corstens FH (2002)  $^{131}\text{I}$ -cG250 monoclonal antibody immunoscintigraphy versus  $^{18}\text{F}$ FDG-PET imaging in patients with metastatic renal cell carcinoma: a comparative study. *Nucl Med Commun* 23:229–236
- Bydder GM (1987) Clinical application of gadolinium-DTPA. In: Stark DD, Bradley WG (eds) *Magnetic resonance imaging*. Mosby, St Louis, pp 182–200
- Condon B, Hadley DM, Hodgson R (2001) The ferromagnetic pillow: a potential MR hazard not detectable by a hand-held magnet. *Br J Radiol* 74:847–851
- Del Sole A, Moncayo R, Tafuni G, Lucignani G (2004) Position of nuclear medicine techniques in the diagnostic work-up of brain tumors. *Q J Nucl Med Mol Imaging*. 48:76–81
- Di Matteo G, Peparini N, Maturo A, Di Matteo FM, Zeri KP, Redler A, Mascagni D (2001) Lateral pelvic lymphadenectomy and total nerve sparing for locally advanced rectal cancer in Western patients. *Panminerva Med* 43:95–101
- Hunter WM, Greenwood FC (1962) Preparation of iodine,  $^{131}\text{I}$ -labelled human growth hormone of high specific activity. *Nature* 194:495–496
- Jani AB, Blend MJ, Hamilton R, Brendler C, Pelizzari C, Krauz L, Sapra B, Vijayakumar S, Awan A, Weichselbaum RR (2004) Radioimmunoscintigraphy for postprostatectomy radiotherapy: analysis of toxicity and biochemical control. *J Nucl Med* 45:1315–1322
- Kitamura K, Takahashi T, Yamaguchi T, Yokota T, Noguchi A, Amagai T, Imanishi J (1989) Immunochemical characterization of the antigen recognized by the murine monoclonal antibody A7 against human colorectal cancer. *Tohoku J Exp Med*. 157:83–93
- Mendonca-Diasand MH, Lauterbur PC (1986) Biological trace elements research. *Magn Reson Med* 3: 328–330
- Molday RS, Yen SPS, Rembaum A (1977) Application of magnetic microspheres in labelling and separation of cells. *Nature* 268:437–438
- Nakada K, Sakamoto J, Watanabe T, Itoh K, Akiyama S, Takagi H (1997) Imaging of recurrent intestinal carcinoma with indium-111-labeled anti-carcinoembryonic antigen CEA102. *Jpn J Cancer Res* 88:605–613
- Oriuchi N, Watanabe N, Sugimachi S, Higuchi T, Imai K, Yamanaka H, Hashimoto M, Kanda H, Endo K (1996) Different biodistribution of  $^{99\text{m}}\text{Tc}$ -labelled chimeric mouse-human monoclonal antibody between athymic mice model and human. *Br J Cancer* 73:1466–1472
- Otsuji E, Yamaguchi Y, Yamaguchi N, Koyama K, Imanishi J, Yamaoka N, Takahashi T (1992) Expression of the cell surface antigen detected by the monoclonal antibody A7 in pancreatic carcinoma cell lines. *Jpn J Surg* 22:351–356
- Otsuji E, Tsuruta H, Toma A, Kobayashi S, Okamoto K, Yata Y, Yamagishi H (2003) Effects of idiotypic human anti-mouse antibody against in vitro binding and antitumor activity of a monoclonal antibody-drug conjugate. *Hepato Gastroenterol* 50: 380–384
- Phom H, Kumar A, Tripathi M, Chandrashekar N, Choudhry VP, Malhotra A, Bal CS (2004) Comparative evaluation of Tc-99 m-heat-denatured RBC and Tc-99 m-anti-D IgG opsonized RBC spleen planar and SPECT scintigraphy in the detection of accessory spleen in post splenectomy patients with chronic idiopathic thrombocytopenic purpura. *Clin Nucl Med* 29:403–409
- Renshaw PF, Owen CS, McLaughlin AC, Frey TG, Leigh JS (1986) Ferromagnetic contrast agents: a new approach. *Magn Reson Med* 3:217–225
- Saini S, Stark DD, Hahn PF, Bousquet JC, Introcasso J, Wittenberg J, Brady TJ, Ferrucci JT (1987) Ferrite particles: A superparamagnetic MR contrast agent for enhanced detection of liver carcinoma. *Radiology* 162:217–222
- Schoeffl GI (1963) Studies on inflammation. III. Growing capillaries: their structure and permeability. *Viwchow's Arch Path Anat* 337:97–141
- Seneterre E, Weissleder R, Jaramillo D, Reimer P, Lee AS, Brady TJ, Wittenberg J (1991) Bone marrow: Ultrasmall superparamagnetic iron oxide for MR imaging. *Radiology* 179:529–533
- Stark DD, Weissleder R, Elizondo G, Hahn PF, Saini S, Todd LE, Wittenberg J, Ferrucci JT (1988) Superparamagnetic iron oxide: clinical application as a contrast agent for MR imaging of the liver. *Radiology* 168:297–301
- Takahashi T, Yamaguchi T, Kitamura K, Noguchi A, Honda M, Otsuji E (1993) Follow-up study of patients treated with monoclonal antibody-drug conjugate: report of 77 cases with colorectal cancer. *Jpn J Cancer Res* 84:976–981
- Weissleder R, Elizondo G, Wittenberg J, Rabiato CA, Begele HH, Josephson L (1990) Ultrasmall superparamagnetic iron oxide: An intravenous contrast agent for assessing lymph nodes with MR imaging. *Radiology* 175:494–498